

Accepted Manuscript

Small Molecule Inhibitors of Bacterial Transcription Complex Formation

Daniel S. Wenholz, Ming Zeng, Cong Ma, Marcin Mielczarek, Xiao Yang, Mohan Bhadbhade, David St.C. Black, Peter J. Lewis, Renate Griffith, Naresh Kumar

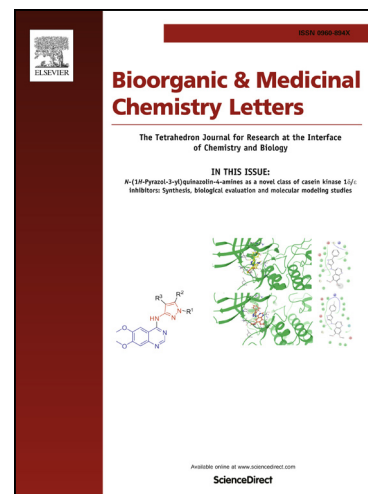
PII: S0960-894X(17)30835-1
DOI: <http://dx.doi.org/10.1016/j.bmcl.2017.08.036>
Reference: BMCL 25230

To appear in: *Bioorganic & Medicinal Chemistry Letters*

Received Date: 19 July 2017
Revised Date: 16 August 2017
Accepted Date: 16 August 2017

Please cite this article as: Wenholz, D.S., Zeng, M., Ma, C., Mielczarek, M., Yang, X., Bhadbhade, M., Black, D.S., Lewis, P.J., Griffith, R., Kumar, N., Small Molecule Inhibitors of Bacterial Transcription Complex Formation, *Bioorganic & Medicinal Chemistry Letters* (2017), doi: <http://dx.doi.org/10.1016/j.bmcl.2017.08.036>

This is a PDF file of an unedited manuscript that has been accepted for publication. As a service to our customers we are providing this early version of the manuscript. The manuscript will undergo copyediting, typesetting, and review of the resulting proof before it is published in its final form. Please note that during the production process errors may be discovered which could affect the content, and all legal disclaimers that apply to the journal pertain.



Small Molecule Inhibitors of Bacterial Transcription Complex Formation

Daniel S. Wenholz^a, Ming Zeng^a, Cong Ma^{b,c}, Marcin Mielczarek^a, Xiao Yang^{b,e}, Mohan Bhadbhade^a, David St. C. Black^a, Peter J. Lewis^b, Renate Griffith^d, and Naresh Kumar^{a,b}*

^a School of Chemistry, UNSW Sydney, Kensington, NSW 2052, Australia

^b School of Environmental and Life Sciences, University of Newcastle, Callaghan, NSW 2308, Australia

^c Department of Applied Biology and Chemical Technology, The Hong Kong Polytechnic University, Hong Kong

^d School of Medical Sciences, UNSW Sydney, Kensington, NSW 2052, Australia

^e Australian Centre for Nanomedicine, UNSW Sydney, Kensington, NSW 2052, Australia

These authors contributed equally.

ABSTRACT

Knoevenagel condensation was employed to generate a set of molecules potentially capable of inhibiting the RNA polymerase- σ^{70}/σ^A interaction in bacteria. Synthesis was achieved *via* reactions between a variety of indole-7-carbaldehydes and rhodanine, *N*-allylrhodanine, barbituric acid or thiobarbituric acid. A library of structurally diverse compounds was examined by enzyme-linked immunosorbent assay (ELISA) to assess the inhibition of the

targeted protein-protein interaction. Inhibition of bacterial growth was also evaluated using *Bacillus subtilis* and *Escherichia coli* cultures. The structure-activity relationship studies demonstrated the significance of particular structural features of the synthesized molecules for RNA polymerase- σ^{70}/σ^A interaction inhibition and antibacterial activity. Docking was investigated as an *in silico* method for the further development of the compounds.

Keywords: Antibacterial activity; Bacterial Transcription; RNA Polymerase; Structure-activity relationship (SAR); Indole

The introduction of antibiotics to medicine has allowed the efficient treatment of bacterial infections posing a substantial threat to human health and life.¹ This revolutionary progress is now under threat by the emergence of bacterial resistance to antibiotics due to their excessive and often unjustified use.¹⁻⁸ The rapidly developing antibiotic resistance problem among highly pathogenic species is significantly escalated by continuously decreasing numbers of new antibacterial drug candidates reaching the market.^{1,3,7-9} Novel antibacterial agents that can undergo successful development towards efficient antibiotics are urgently needed in order to counteract the dramatically intensifying bacterial resistance to currently used drugs.^{3,9}

A key priority of antibacterial drug research is the identification of molecules exhibiting novel mechanisms of activity rather than the development of existing classes of antibiotics to which resistance has already occurred.^{3,9} Bacterial metabolic pathways, especially the gene expression processes, have been exploited as attractive drug targets.¹⁰ One of the most promising directions to explore is targeting bacterial transcription,¹⁰⁻¹¹ the process of transcribing genetic information encoded in DNA into RNA *via* the enzyme RNA polymerase (RNAP).¹⁰ Two forms of DNA-dependent RNAP are present in bacterial cells: the core enzyme and the holoenzyme (HE).¹²⁻¹⁶ The HE is formed between the RNAP core enzyme, which consists of five subunits ($\alpha_2\beta\beta'\omega$), and a transcription factor, such as a σ factor, giving the enzyme transcription specificity by allowing it to recognize promoter sites on the DNA.¹²⁻

¹⁷ Whilst a wide range of σ factors exist both within and between bacterial species, an essential σ factor, σ^A in Gram-positive *B. subtilis* and σ^{70} in Gram-negative *E. coli*, is involved in the transcription of ‘housekeeping’ genes.^{12, 17-18}

A novel antibacterial strategy seeks to inhibit HE formation *via* disruption of the protein-protein interaction (PPI) that occurs at the binding ‘hotspot’ between the highly conserved solvent-exposed clamp helix (CH) region of the β' subunit of the RNAP core and region 2.2 of the σ^{70}/σ^A factor,^{12-13, 19} and thus inhibit bacterial transcription. As the σ^{70}/σ^A factors demonstrate high structural similarity across a variety of bacteria species,^{10, 17} compounds that inhibit the β' -CH- $\sigma^{70}/\sigma^A_{2.2}$ interaction are expected to show broad spectrum activity. Additionally, since σ^{70}/σ^A factors regulate transcription initiation only in bacterial cells,¹³ drugs targeting this PPI would be less likely to produce adverse effects.

Recently a series of benzoic acid-based molecules has been synthesized and evaluated for transcription inhibitory activity, with compounds **1**, **2**, **3** and **4** (Figure 1) efficiently inhibiting the interaction between core RNAP and σ^{70} , exhibiting 85-100% transcription inhibition at 10 μM .²⁰⁻²¹ Additionally, molecule **1** proved to be a good broad spectrum inhibitor of bacterial growth showing MIC values of 12.5 and 6.25 $\mu\text{g/mL}$ against *Staphylococcus epidermidis* and *E. coli*, respectively.²⁰

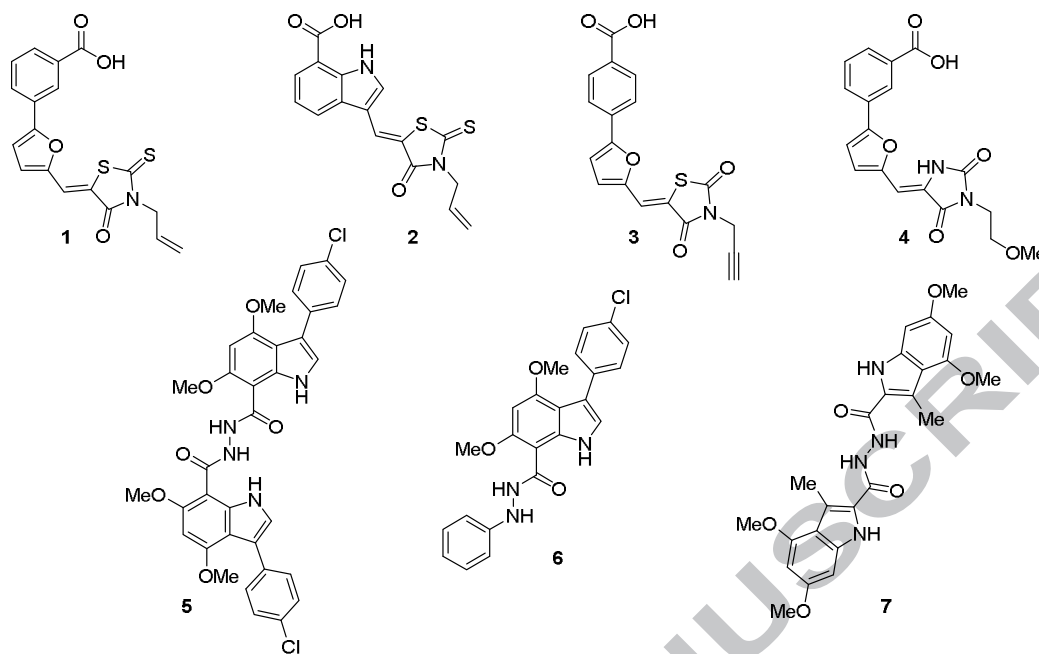


Figure 1. Highly active synthetic compounds inhibiting transcription initiation in bacteria.²⁰

22-24

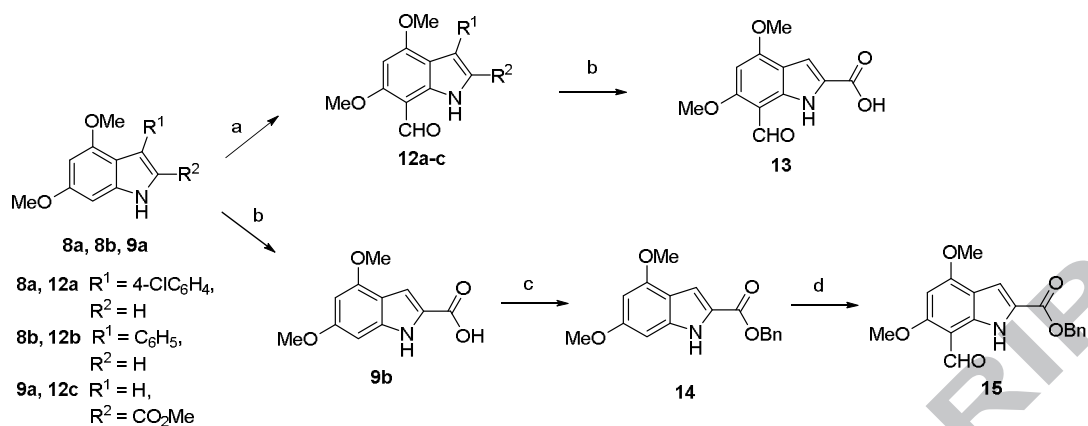
The pharmacophore model previously developed by our group based on a *B. subtilis* RNAP homology model and the amino acids in σ^A found in mutagenesis studies to be responsible for the RNAP HE formation^{19, 24} was used for the design of several classes of structurally related indole-based inhibitors of the β' -CH- $\sigma^A_{2.2}$ interaction such as bis-indole GKL003 **5** (Figure 1).²²⁻²⁴ In our preliminary studies involving isothermal titration calorimetry experiments, the bis-indoles were found to inhibit transcription by competitively binding to the β' -CH region of the RNAP core enzyme.²⁴ Through the use of ELISA GKL003 **5** was determined to inhibit the PPI between β' -CH and *B. subtilis* σ^A by 63% at 15 μM .²⁵ Further development of this series led to molecules **6** and **7** (Figure 1) as the most potent mono- and bis-indole-based inhibitors, with of 86% and 60% inhibition of the β' -CH- σ^A PPI at 15 μM as measured by ELISA, respectively, and they inhibited *E. coli* growth at 200 μM (16% and 21% inhibition, respectively).²²⁻²³

The structure-activity relationship (SAR) studies performed on a large family of compounds related to **1-4** showed that incorporation of a carboxylic acid group significantly increased their inhibitory activity against the β' -CH- σ^{70} interaction.²⁰ Moreover, the allylrhodanine moiety was found to be essential for antibacterial activity.²⁰ These observations were used to design a series of mono-indole compounds based upon the structures of **6** and **7** that incorporated features of **1-4**. A focus was placed on including compounds with lower molecular weight and increased polarity in order to overcome the solubility issues encountered by the previous compounds.^{22-23, 25} These compounds were synthesized and evaluated for their ability to inhibit the interaction between the β' -CH region of RNAP core and σ^A factor by ELISA, and for antibacterial activity against *B. subtilis* and *E. coli*. Biological evaluation was followed by molecular docking and SAR studies.

The indoles **8a** and **8b** were obtained following the well-established Bischler indole synthesis modified by our group.²⁶⁻²⁷ The methyl 4,6-dimethoxyindole-2-carboxylate **9a** was afforded *via* the Hemetsberger indole synthesis.²⁸ The indoles **8a**, **8b** and **9a** were formylated under Vilsmeier-Haack conditions at position 7 (Scheme 1) to give the corresponding indole-7-carbaldehydes **12a-c** in yields of 85-95%.²⁹ The methyl ester **12c** was also converted into the carboxylic acid **13** *via* alkaline hydrolysis in 95% yield (Scheme 1).

In order to synthesize the benzyl ester **15**, the methyl indole-2-carboxylate **9a** was first hydrolyzed to the indole-2-carboxylic acid **9b**³⁰ using a solution of potassium hydroxide in an ethanol/water mixture, followed by DCC-mediated coupling reaction between the acid **9b** and benzyl alcohol in the presence of DMAP as a catalyst to give the benzyl indole-2-carboxylate **14** in 35% yield. Subsequent Vilsmeier-Haack formylation of the ester **14** furnished indole-7-carbaldehyde **15** in 90% yield (Scheme 1).

Scheme 1. Synthesis of compounds **9b**, **12-15**.



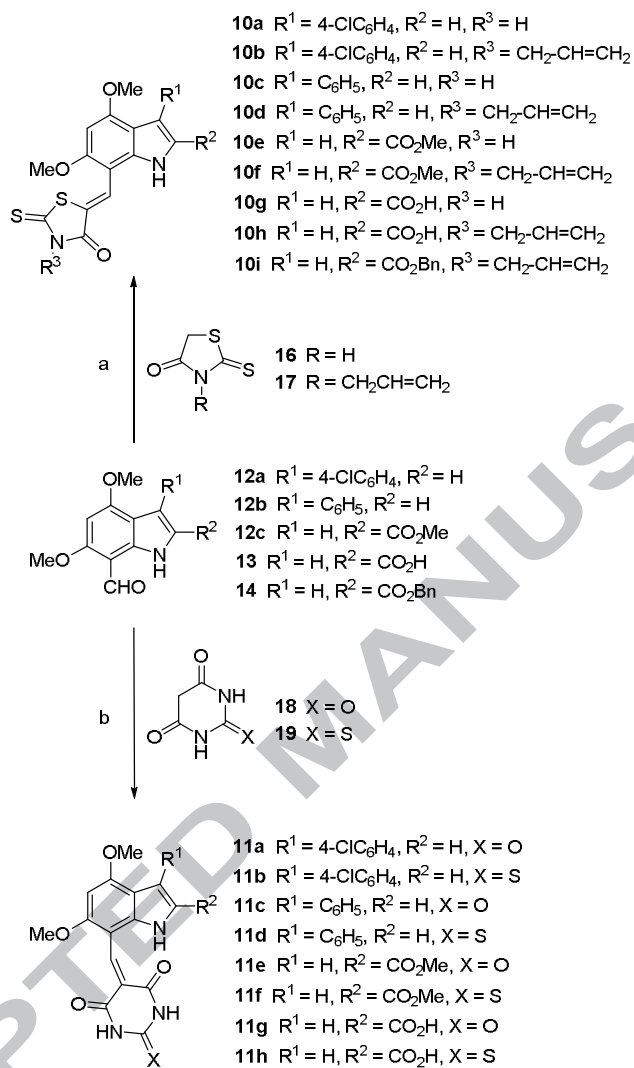
(a) POCl₃ (1.0 equiv), DMF, 0 °C • room temp., 2 h, 85-95%; (b) KOH (excess), EtOH/H₂O 3:1 (v/v), reflux, 2 h, 95-99%; (c) BnOH (1.2 equiv), DCC (3.0 equiv), DMAP (0.2 equiv), DCM, 0 °C • room temp., 3 h, 35%; (d) POCl₃ (1.1 equiv), DMF, 0 °C • room temp., 12 h, 99%.

The reaction between indole-7-carbaldehyde **12a** and rhodanine **16** was carried out in a 1:1 molar ratio in the presence of piperidine as a catalyst by heating in anhydrous ethanol under reflux. However, as indicated by TLC analysis, even after 72 h the reaction did not proceed to completion. In order to shift the reaction equilibrium towards the formation of the product **10a**, the amount of rhodanine was increased to 1.2 equivalents along with the addition of β -alanine (2 equiv) and glacial acetic acid as a solvent.³¹ TLC analysis showed that the starting indole-7-carbaldehyde **12a** had been fully consumed after 3 h of heating under reflux. As the product of the reaction was found to be very insoluble in the majority of commonly used solvents such as EtOAc, EtOH or DCM, column chromatography was excluded as a potential method for its purification. Therefore, a number of solvent mixtures were tested to recrystallize the crude product. A DMF/MeOH mixture was finally used for recrystallization to give the compound **10a** as a dark red powder in 60% yield (Scheme 2). This method was applied to the reactions of the indole-7-carbaldehydes **12b**, **12c**, **13** and **15** with rhodanine **16** or allylrhodanine **17** to afford the desired products **10a-i** in 30-68% yield (Scheme 2). The ¹H

NMR spectra of the products display a characteristic singlet at around 7.80-8.50 ppm which indicates the successful formation of the double bond linker.

The single crystal X-ray crystallographic analyses confirmed (*Z*)-stereochemistry of the molecules **10c** and **10d** (Figure 2). This observation is in a good agreement with literature data.³²⁻³³

The Knoevenagel condensations between indole-7-carbaldehydes **12a-c** or **13** and barbituric acid **18** or thiobarbituric acid **19** resulted in the formation of the compounds **11a-h** as dark red powders in 27-100% yield after recrystallization from a DMF/MeOH mixture (Scheme 2).³⁴ The reactions were found to proceed efficiently by heating the substrates in either an acetic anhydride/acetic acid 1:10 mixture or in acetic anhydride under reflux for 2 h. Furthermore, the use of a catalyst was not crucial for these reactions.

Scheme 2. Synthesis of compounds **10a-i** and **11a-h**.

(a) β -Alanine (2 equiv), $\text{CH}_3\text{CO}_2\text{H}$, $100\text{ }^\circ\text{C}$, 3 h (30-68%); (b) acetic anhydride or acetic anhydride and $\text{CH}_3\text{CO}_2\text{H}$, $90\text{ }^\circ\text{C}$, 2 h (27-100%).

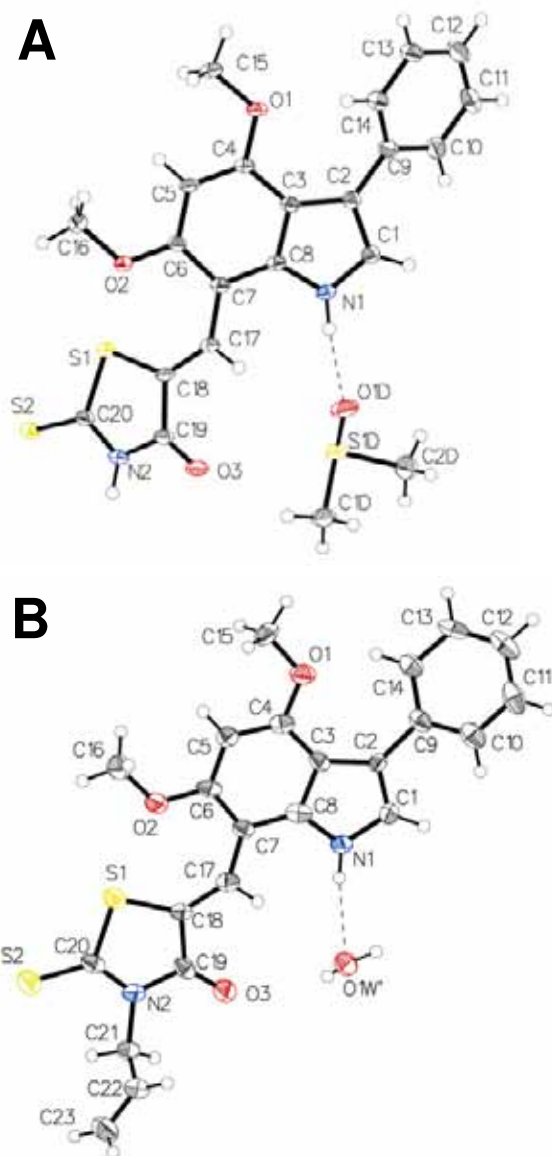


Figure 2. ORTEP diagrams of the crystal structures of the compounds **10c** (A) and **10d** (B) (front view, 50% probability thermal ellipsoids at 100 K shown).

The library of the seventeen synthesized molecules was evaluated for biological activity. Firstly, the inhibition of the interaction between *B. subtilis* σ^A and the β' -CH region of the core RNAP was examined by ELISA at 15 μM compound concentration and is expressed as a percentage of the positive control (interaction between σ^A and β' -CH in the absence of the inhibitor) where the positive control interaction is 100%. Secondly, bacterial growth

inhibition was evaluated at 0.2 mM compound concentration using two representative species, *B. subtilis* (Gram-positive) and *E. coli* (Gram-negative), and is expressed as a percentage of the positive control (bacterial growth in the absence of the inhibitor) where the positive control bacterial growth is 100% (Table 1).²²⁻²⁵

Table 1. Evaluation of antibacterial activity of the synthesized molecules.

Entry	clog P	MW	β' -CH- σ^A interaction inhibition at 15 μ M by ELISA [%]	Growth inhibition of <i>E. coli</i> at 0.2 mM [%]	Growth inhibition of <i>B. subtilis</i> at 0.2 mM [%]
10a	5.3	430.9	21	15	0
10b	6.1	471.0	34	14	8
10c	4.6	396.5	17	45 ^a	44 ^a
10d	5.4	436.5	0	66	44
10e	3.3	378.4	3	28	45
10f	4.1	418.5	46	79 ^b	22
10g	3.0	364.4	36	26	0
10h	3.9	404.5	74	30	21
10i	5.7	494.6	63	28	6
11a	3.3	425.8	15	30 ^a	41 ^a
11b	4.2	441.9	14	24	0
11c	2.6	391.4	45	0	83
11d	3.5	407.4	14	0	0
11e	1.3	373.3	28	20	89 ^b
11f	2.2	389.4	17	57	91 ^b
11g	1.1	359.3	28	0	0
11h	2.0	375.4	71	0	0
12	5.2	447.5	21	53	0

^a precipitation at 0.2 mM, ^b affects the exponential phase of bacterial growth.

The top three hits (**10h**, **10i** and **11h**) exhibited greater than 60% inhibition of the β' -CH- σ^A interaction in the ELISA assay at 15 μ M (74%, 63% and 71%, respectively). However, **11h** was found to be inactive against both *E. coli* and *B. subtilis*, whilst **10h** and **10i** showed moderate and low antibacterial activity.

Although compound **10f** possessed only moderate β' -CH- σ^A inhibition of 46 % at 15 μ M, it showed good antibacterial activity against *E. coli*, with growth inhibition of 79% and moderate activity against *B. subtilis*, showing potential for further development as an antibacterial agent, particularly against Gram-negative bacteria. Similarly, compound **11c** displayed only moderate inhibition of the PPI but inhibited the growth of *B. subtilis* (83% at

0.2 mM), but showed no effect on *E. coli* growth. The molecules with high antibacterial activity, but very low RNAP- σ inhibitory activity, such as **11e** and **11f** (89% and 91% inhibition of *B. subtilis* growth at 0.2 mM, respectively) might exhibit antibacterial activity *via* additional mechanisms different from inhibition of the β' -CH- σ^A interaction. However, compounds **10f**, **11e** and **11f** were observed to affect the exponential phase of bacterial growth and this suggests that they inhibit transcription.²⁴

To investigate potential problems of the compounds in reaching their targets, calculated logP values and molecular weights are provided in Table 1. Both values are high for **10i** and **10b**, possibly explaining the low growth inhibition observed, however, this is not the case for **10g**, **10h**, **11g** and **11h**, all of which however, contain ionizable COOH groups that may prevent efficient uptake by the bacteria. Compound **10d** is very lipophilic, and this combined with the fact that it does not inhibit the PPI, suggests a different mechanism of growth inhibition. The compounds all incorporate substructures similar to those of the literature compounds as exemplified by **1-4**. These exhibited antibacterial activity against a mutated *E. coli* strain deficient in multidrug efflux systems, but not against wild-type *E. coli*.^{20, 35} They have also been shown to have off-target effects.³⁵ These issues could be related to the presence of common interference substructures (PAINS)³⁶ and will need to be investigated further in the development of the compounds presented here. However, we have previously not observed any interference in several detailed assays of compound **5** at different concentrations.²⁴

The synthesized compounds, **10a-i** and **11a-k**, were docked using Genetic Optimized Ligand Docking (GOLD) through the Discovery Studio (DS) interface onto the β' -CH region of a new RNAP homology model. This was repeated with the most active compound from the SB series, **1**, as well as the three active compounds from the GKL series, **5**, **6** and **7**.^{20, 22-23, 25} Compounds with carboxylic acid groups were also docked in their negatively ionized

deprotonated state. As the solvent exposed residue side chains are not static in the core enzyme, it was deemed to be important to allow flexibility in the amino acid side chains in and around the binding hotspot area.³⁷ The side chains of the residues in the PPI hotspot on β' -CH²⁴ were set to flexible in the docking protocol, allowing transient pockets or grooves to appear in the relatively flat β' -CH surface to facilitate greater interaction with small molecules.

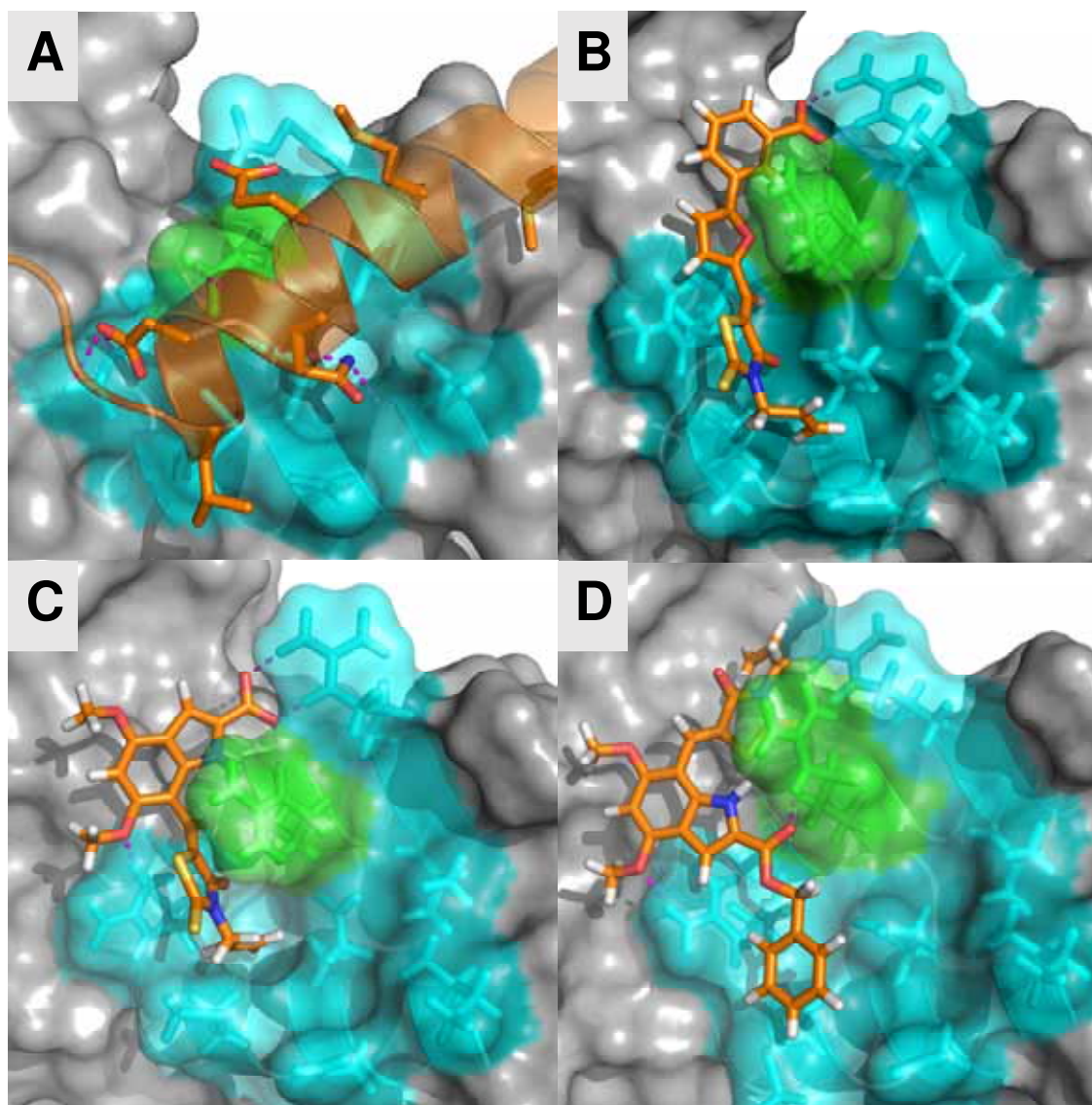


Figure 3. Positions and intermolecular interactions of $\sigma^A_{2.2}$ and docked compounds at the β' -CH binding hotspot²⁴ of a *B. subtilis* RNAP holoenzyme homology model. Hotspot residues coloured in cyan, a critical Arg267 residue in green, and hydrogen bond interactions are shown as magenta dashed lines. (A) σ^A 2.2 region in homology model of HE. (B) Docked **1(1)**. (C) Docked **10h(1)**. (D) Docked **10i**. **(1)** indicates deprotonated carboxylic acid group.

Table 3. Docking results for synthesized compounds and known inhibitors.

Entry	Carboxylic Acid Group State	Docking GOLD Score
10a	-	49.2
10b	-	51.8
10c	-	52.1
10d	-	45.3
10e	-	50.7
10f	-	54.2
10g	COOH	55.5
10g(1)	COO ⁻	66.2
10h	COOH	54.8
10h(1)	COO ⁻	71.2
10i	-	63.6
10j	-	50.4
11a	-	42.7
11b	-	45.7
11c	-	47.3
11d	-	51.0
11e	-	51.4
11f	-	50.8
11g	COOH	47.8
11g(1)	COO ⁻	62.0
11h	COOH	51.2
11h(1)	COO ⁻	70.7
1	COOH	59.6
1(1)	COO ⁻	67.6
5	-	74.1
6	-	56.3
7	-	68.0

It was observed that the majority of the docked compounds were placed by GOLD into a groove running between Arg264 and Arg267 on the β^1 -CH region, as shown in Figure 3. Although this position does not cover the entire hotspot area, it does allow strong interactions with the three arginine residue that are most important in the PPI, namely Arg264, Arg267 and Arg270 as identified from mutagenesis data.²⁴ This position also has great potential to interrupt interactions with the σ^A -Glu277 residue, which has been identified as playing an important role in the PPI as part of the $\sigma_{2.2}^A$ hotspot.¹⁹

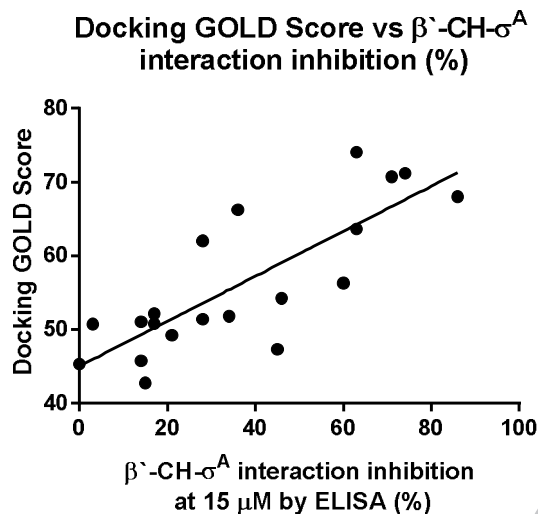


Figure 4. Relationship between docking GOLD scores and β' -CH- σ^A interaction inhibition of synthesized compounds **10a-i** and **11a-h** along with known active inhibitors **5-7**.²²⁻²⁴

The compounds were mapped to the published pharmacophore from our group²⁴ (data not shown), however, no level of correlation with the biological data was observed. In comparison to the pharmacophore mapping results, there was good correlation between the β' -CH- σ^A inhibition activities and the highest GOLD score of each compound ($R^2 = 0.64$), taking into account the structural diversity of the compounds (Figure 4). Furthermore, the two compounds with the highest β' -CH- σ^A inhibitory activities, **10h** and **11h**, achieved the two highest GOLD scores of 71.2 and 70.7, respectively. The high GOLD scores observed also suggest that the ELISA results were likely due to strong interaction with the β' -CH region, rather than being artifacts of interference compounds. Although the high GOLD scores for **10h** and **11h** were only obtained by the ionised forms of both compounds, the non-ionisable compound with the highest β' -CH- σ^A inhibition, **10i**, also achieved the best docking result of all neutral synthesized compounds with a GOLD score of 63.6. This trend was also seen with the known inhibitors, **1**, **5** and **7**, the docking results of which all showed GOLD scores close to 70. With a GOLD score of 56.3, mono-indole **6** scored the lowest out of the known

inhibitors, consistent with it exhibiting the lowest β' -CH- σ^A inhibition of the four.²³ These results show that docking shows potential as a tool in the future development of RNAP HE formation inhibitors.

The β' -CH- σ^A inhibitory activities and antibacterial activities along with the docking results of the synthesized molecules were also analyzed for possible structure-activity relationships. It was observed that the replacement of the 3-phenyl and 3-(4'-chlorophenyl) group with a carboxylic acid or ester at the 2-position of the indole backbone led to greatly increased ability to inhibit the β' -CH- σ^A interaction, as can be seen in a comparison between the β' -CH- σ^A inhibitory activities of **11b** and **11d** with **11h**. This was further supported by the predicted binding modes from the docking analysis, wherein the carboxylic acid and ester groups at the 2-position were predicted to form hydrogen bonds with Arg267 and Arg270 (Figure 3), whilst no interaction was predicted for the phenyl groups at the 3-position with the protein. This was consistent with the fact that both the 3-phenyl group and the 3-(4'-chlorophenyl) group were unable to map to any feature on the pharmacophore. These observations show that the 3-phenyl group is not essential for the antibacterial activity of the compounds.

It was also observed that a carboxylic acid group at the 2-position of the indole system produced much higher β' -CH- σ^A inhibitory activities than those observed for the esters at this position. This is apparent when comparing the β' -CH- σ^A inhibitory activities of **10f** with **10j** (46% and 74%, respectively) or **11f** with **11h** (17% and 71%, respectively). This may be due to the carboxylic acid group's ability to ionize and form charge-charge interactions with the arginine groups of the binding hotspot, typically Arg270, as suggested by the docking results. However, the incorporation of a CO₂Me group at the 2-position improved antibacterial activity. This is shown in the comparison of compounds **10h** and **10f**, where inhibition of the *E. coli* growth increased from 30% to 79% or the compounds **10i** and **10e**, where inhibition of the *B. subtilis* growth increased from 6% to 45% when the CO₂H group was replaced by the

CO₂Me group. Moreover, such a replacement resulted in a dramatic increase in antibacterial activity against both *E. coli* and *B. subtilis* for the molecules **11g** and **11e**, or **11h** and **11f**. Notably, the CO₂Me group was present in all the inhibitors that affected the exponential phase of bacterial growth (**10f**, **11e** and **11f**). This may be due to the increase in clogP of the esters, allowing greater passive diffusion through the bacterial cell membrane.

It was observed that the RNAP- σ inhibitory activity of the esters could be improved by replacing the CO₂Me group with a larger CO₂Bn group, as shown *via* comparison of **10f** and **10i**. This change increased the β' -CH- σ^A inhibitory activity from 46% to 63%, which may be the result of an increase in hydrophobic interactions. This is in agreement with the docking results, which show the benzyl ring interacting with Met287 with a different predicted mode of binding to the other esters (Figure 3). However, this modification resulted in a decrease in antibacterial activity, possibly due to the increase in molecular weight resulting in a reduction in passive transport through bacterial membranes. This result highlights a potential future direction in modification of the ester group with other less bulky, less hydrophobic groups.

Comparison of the activities of the molecules **10g**, **10h**, **11g** and **11h** indicates that the allylrhodanine (present in the molecule **10h**) is most beneficial for RNAP- σ inhibitory activity among the 5- and 6-membered heterocyclic rings. The *N*-allyl group of allylrhodanine **17** is important not only for RNAP- σ inhibitory activity, but also for antibacterial activity as highlighted in the case of the compounds **10e** and **10f**.

In conclusion, 17 novel compounds were successfully synthesized utilizing Knoevenagel condensation. The ability of the compounds to inhibit the interaction between $\sigma^A_{2.2}$ and the β' -CH region of the core RNAP was evaluated by ELISA at 15 μ M. Antibacterial activity of the molecules was determined based on the inhibition of *E. coli* and *B. subtilis* growth in culture at 0.2 mM. The compounds were then docked onto the solvent exposed face of the β' -CH region of a *B. subtilis* σ^A homology model using GOLD. The SAR studies supported by the

molecular docking resulted in the identification of molecular features potentially beneficial for inhibition of the β' -CH- σ^A interaction and bacterial growth. Modifications of the ester group at the C2 position of the indole are a promising direction for the design of compounds that exhibit high inhibition of both the RNAP- σ assembly formation and bacterial growth. In particular, a methyl group could be replaced with ethyl, *n*-propyl or *iso*-propyl groups as the larger ester groups could enhance RNAP- σ inhibitory activity as observed for the benzyl ester. As confirmed by calculation of molecular properties and much fewer solubility-related issues encountered during the examination of antibacterial activity, this research has delivered compounds with significantly improved aqueous solubility compared to the previously synthesized bis-indoles^{22,25} and mono-indoles²³. This is mainly due to reduction of molecular weight and size, and increase in hydrophilicity by the incorporation of polar groups such as the carboxylic group. Furthermore, this study has demonstrated that *in silico* docking using GOLD shows potential as a tool for the further development of RNAP- σ inhibitors and future studies may benefit immensely through implementation of this technique during lead development.

Acknowledgments

This work was supported by a Project Grant from the National Health and Medical Research Council (NHMRC) Australia to N.K., P.L. and R.G. [NHMRC Grant APP1008014]. M.M. is thankful to UNSW Australia for a Tuition Fee Scholarship (TFS) and to N.K. for a Living Allowance Scholarship. We would like to give a special thank you to Thanh Le, Oscar Thach, Samuel K. Kutty and Murat Bingul for their aid in this study. We are also thankful to the Nuclear Magnetic Resonance Facility and the Bioanalytical Mass Spectrometry Facility (BMSF) in the Mark Wainwright Analytical Centre at UNSW Australia for the opportunity of using their instruments.

Abbreviations Used

CH, clamp helix; DOPE, Discrete Optimized Protein Energy; DS, Discovery Studio; GOLD, Genetic Optimized Ligand Docking; HE, holoenzyme; PPI, protein-protein interaction; PDF, probability density function; RMSD, root mean-square-deviation; RNAP, RNA polymerase.

REFERENCES

1. Hart, C., Antibiotic resistance: an increasing problem? *Br. Med. J.* **1998**, *316* (7140), 1255-1257.
2. Yoshikawa, T. T., Antimicrobial resistance and aging: beginning of the end of the antibiotic era? *J. Am. Geriatr. Soc.* **2002**, *50* (s7), 226-229.
3. Shekhar, C., Bacteria: Drug Resistance Spreads, but Few New Drugs Emerge. *Chem. Biol.* **2010**, *17* (5), 413-414.
4. Neu, H. C., The crisis in antibiotic resistance. *Science* **1992**, *257* (5073), 1064-1074.
5. Mazel, D.; Davies, J., Antibiotic resistance in microbes. *Cell. Mol. Life Sci.* **1999**, *56* (9), 742-754.
6. McAdam, A. J.; Hooper, D. C.; DeMaria, A.; Limbago, B. M.; O'Brien, T. F.; McCaughey, B., Antibiotic resistance: how serious is the problem, and what can be done? *Clin. Chem.* **2012**, *58* (8), 1182-1186.
7. Peleg, A. Y.; Hooper, D. C., Hospital-acquired infections due to gram-negative bacteria. *N. Engl. J. Med.* **2010**, *362* (19), 1804-1813.
8. Boucher, H. W.; Talbot, G. H.; Bradley, J. S.; Edwards, J. E.; Gilbert, D.; Rice, L. B.; Scheld, M.; Spellberg, B.; Bartlett, J., Bad bugs, no drugs: no ESKAPE! An update from the Infectious Diseases Society of America. *Clin. Infect. Dis.* **2009**, *48* (1), 1-12.
9. Chopra, I., The 2012 Garrod Lecture: Discovery of antibacterial drugs in the 21st century. *J. Antimicrob. Chemother.* **2012**, *68*, 496-505.
10. Villain-Guillot, P.; Bastide, L.; Gualtieri, M.; Leonetti, J.-P., Progress in targeting bacterial transcription. *Drug Discov. Today* **2007**, *12* (5), 200-208.

11. Ma, C.; Yang, X.; Lewis, P. J., Bacterial Transcription as a Target for Antibacterial Drug Development. *Microbiol. Mol. Biol. Rev.* **2016**, *80* (1), 139-160.
12. Vassylyev, D. G.; Sekine, S.-i.; Laptenko, O.; Lee, J.; Vassylyeva, M. N.; Borukhov, S.; Yokoyama, S., Crystal structure of a bacterial RNA polymerase holoenzyme at 2.6 Å resolution. *Nature* **2002**, *417* (6890), 712-719.
13. Burgess, R. R.; Anthony, L., How sigma docks to RNA polymerase and what sigma does. *Curr. Opin. Microbiol.* **2001**, *4* (2), 126-131.
14. Finn, R. D.; Orlova, E. V.; Gowen, B.; Buck, M.; van Heel, M., Escherichia coli RNA polymerase core and holoenzyme structures. *EMBO J.* **2000**, *19* (24), 6833-6844.
15. Patikoglou, G. A.; Westblade, L. F.; Campbell, E. A.; Lamour, V.; Lane, W. J.; Darst, S. A., Crystal structure of the Escherichia coli regulator of σ^{70} , Rsd, in complex with σ^{70} domain 4. *J. Mol. Biol.* **2007**, *372* (3), 649-659.
16. Mekler, V.; Pavlova, O.; Severinov, K., Interaction of Escherichia coli RNA polymerase σ^{70} subunit with promoter elements in the context of free σ^{70} , RNA polymerase holoenzyme, and the σ^{70} - σ^{70} complex. *J. Biol. Chem.* **2011**, *286* (1), 270-279.
17. Malhotra, A.; Severinova, E.; Darst, S. A., Crystal structure of a σ^{70} subunit fragment from E. coli RNA polymerase. *Cell* **1996**, *87* (1), 127-136.
18. Blanco, A. G.; Canals, A.; Bernués, J.; Solà, M.; Coll, M., The structure of a transcription activation subcomplex reveals how σ^{70} is recruited to PhoB promoters. *EMBO J.* **2011**, *30* (18), 3776-3785.
19. Johnston, E. B.; Lewis, P. J.; Griffith, R., The interaction of Bacillus subtilis σ^A with RNA polymerase. *Protein Sci.* **2009**, *18* (11), 2287-2297.

20. Villain-Guillot, P.; Gualtieri, M.; Bastide, L.; Roquet, F.; Martinez, J.; Amblard, M.; Pugniere, M.; Leonetti, J.-P., Structure-activity relationships of phenyl-furanyl-rhodanines as inhibitors of RNA polymerase with antibacterial activity on biofilms. *J. Med. Chem.* **2007**, *50* (17), 4195-4204.
21. André, E.; Bastide, L.; Michaux-Charachon, S.; Gouby, A.; Villain-Guillot, P.; Latouche, J.; Bouchet, A.; Gualtiéri, M.; Leonetti, J.-P., Novel synthetic molecules targeting the bacterial RNA polymerase assembly. *J. Antimicrob. Chemother.* **2006**, *57* (2), 245-251.
22. Mielczarek, M.; Devakaram, R. V.; Ma, C.; Yang, X.; Kandemir, H.; Purwono, B.; Black, D. StC.; Griffith, R.; Lewis, P. J.; Kumar, N., Synthesis and biological activity of novel bis-indole inhibitors of bacterial transcription initiation complex formation. *Org. Biomol. Chem.* **2014**, *12* (18), 2882-2894.
23. Mielczarek, M.; Thomas, R. V.; Ma, C.; Kandemir, H.; Yang, X.; Bhadbhade, M.; Black, D. StC.; Griffith, R.; Lewis, P. J.; Kumar, N., Synthesis and biological activity of novel mono-indole and mono-benzofuran inhibitors of bacterial transcription initiation complex formation. *Bioorg. Med. Chem.* **2015**, *23* (8), 1763-1775.
24. Ma, C.; Yang, X.; Kandemir, H.; Mielczarek, M.; Johnston, E. B.; Griffith, R.; Kumar, N.; Lewis, P. J., Inhibitors of Bacterial Transcription Initiation Complex Formation. *ACS Chem. Biol.* **2013**, *8* (9), 1972-1980.
25. Kandemir, H.; Ma, C.; Kutty, S. K.; Black, D. StC.; Griffith, R.; Lewis, P. J.; Kumar, N., Synthesis and biological evaluation of 2, 5-di (7-indolyl)-1, 3, 4-oxadiazoles, and 2-and 7-indolyl 2-(1, 3, 4-thiadiazolyl) ketones as antimicrobials. *Bioorg. Med. Chem.* **2014**, *22* (5), 1672-1679.

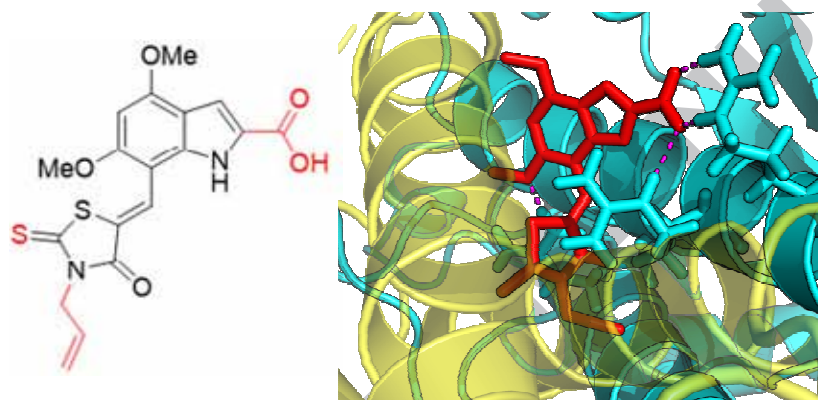
26. Pchalek, K.; Jones, A. W.; Wekking, M. M.; Black, D. StC., Synthesis of activated 3-substituted indoles: an optimised one-pot procedure. *Tetrahedron* **2005**, *61* (1), 77-82.
27. Mitchell, P. S.; Sengul, I. F.; Kandemir, H.; Nugent, S. J.; Chen, R.; Bowyer, P. K.; Kumar, N.; Black, D. StC., Bromination of 4, 6-dimethoxyindoles. *Tetrahedron* **2012**, *68* (39), 8163-8171.
28. Bingul, M.; Cheung, B. B.; Kumar, N.; Black, D. StC., Synthesis of symmetrical and unsymmetrical diindolylmethanes via acid-catalysed electrophilic substitution reactions. *Tetrahedron* **2014**, *70* (40), 7363-7369.
29. Black, D. StC.; Bowyer, M.; KUMAR, N.; Mitchell, P., Calix [3] indoles, new macrocyclic tris (indolylmethylene) compounds with 2, 7-linkages. *J. Chem. Soc. Chem. Commun.* **1993**, (10), 819-821.
30. Black, D. StC.; Kumar, N.; Wong, L., Synthesis of 4, 6-dimethoxyindoles. *Aust. J. Chem.* **1986**, *39* (1), 15-20.
31. Mori, M.; Moraca, F.; Deodato, D.; Ferraris, D. M.; Selchow, P.; Sander, P.; Rizzi, M.; Botta, M., Discovery of the first potent and selective Mycobacterium tuberculosis Zmp1 inhibitor. *Bioorg. Med. Chem. Lett.* **2014**, *24* (11), 2508-2511.
32. Zvezdanovic, J.; Daskalova, L.; Yancheva, D.; Cvetkovic, D.; Markovic, D.; Anderluh, M.; Smelcerovic, A., 2-Amino-5-alkylidene-thiazol-4-ones as promising lipid peroxidation inhibitors. *Monatsh. Chem.* **2014**, *145*, 945-952.
33. Mukhopadhyay, C.; Ray, S., Rapid and straightforward one-pot expeditious synthesis of 2-amino-5-alkylidene-thiazol-4-ones at room temperature. *Tetrahedron Lett.* **2011**, *52* (48), 6431-6438.

34. Klikar, M.; Bureš, F.; Pytela, O.; Mikysek, T.; Padlková, Z.; Barsella, A.; Dorkenoo, K.; Achelle, S., N, N•-Dibutylbarbituric acid as an acceptor moiety in push–pull chromophores. *New J. Chem.* **2013**, *37* (12), 4230-4240.
35. Mariner, K. R.; Trowbridge, R.; Agarwal, A. K.; Miller, K.; O'Neill, A. J.; Fishwick, C. W.; Chopra, I., Furanyl-rhodanines are unattractive drug candidates for development as inhibitors of bacterial RNA polymerase. *Antimicrob. Agents Chemother.* **2010**, *54* (10), 4506-4509.
36. Baell, J. B.; Holloway, G. A., New substructure filters for removal of pan assay interference compounds (PAINS) from screening libraries and for their exclusion in bioassays. *J. Med. Chem.* **2010**, *53* (7), 2719-2740.
37. Wells, J. A.; McClendon, C. L., Reaching for high-hanging fruit in drug discovery at protein–protein interfaces. *Nature* **2007**, *450* (7172), 1001-1009.
38. Bruker *SADABS*, Bruker AXS Inc.: Madison, Wisconsin, USA, 2001.
39. Bruker *APEX2 and SAINT*, Bruker AXS Inc.: Madison, Wisconsin, USA, 2007.
40. Sheldrick, G. M., *Acta Crystallogr.* **2008**, (A64), 112.
41. Dolomanov, O. V.; Bourhis, L. J.; Gildea, R. J.; Howard, J. A.; Puschmann, H., OLEX2: a complete structure solution, refinement and analysis program. *J. Appl. Crystallogr.* **2009**, *42* (2), 339-341.
42. Kabsch, W., Automatic processing of rotation diffraction data from crystals of initially unknown symmetry and cell constants. *J. Appl. Crystallogr.* **1993**, *26* (6), 795-800.
43. Sali, A.; Blundell, T., Comparative protein modelling by satisfaction of spatial restraints. *Protein structure by distance analysis* **1994**, *64*, C86.

44. Chen, J.; Campbell, A. P.; Urmi, K. F.; Wakelin, L. P.; Denny, W. A.; Griffith, R.; Finch, A. M., Human β_1 -adrenoceptor subtype selectivity of substituted homobivalent 4-aminoquinolines. *Bioorg. Med. Chem.* **2014**, *22* (21), 5910-5916.

45. MacDougall, I. J.; Griffith, R., Selective pharmacophore design for β_1 -adrenoceptor subtypes. *J. Mol. Graph. Model.* **2006**, *25* (1), 146-157.

GRAPHIC ABSTRACT



74%
inhibition
of β_1 -CH^A
interaction at
15 μ M